

Corrosion and Tribological Studies of Bamboo Leaf Ash and Alumina Reinforced Al-Mg-Si Alloy Matrix Hybrid Composites in Chloride Medium

K.K. Alaneme^{1,2,*}, P.A. Olubambi³, A.S. Afolabi⁴, M.O. Bodurin¹

¹Department of Metallurgical and Materials Engineering, Federal University of Technology, P.M.B 704, Akure, Nigeria

²Department of Mining and Metallurgical Engineering, University of Namibia, Ongwediva Engineering Campus, Ongwediva, Namibia

³Department of Chemical and Metallurgical Engineering, Tshwane University of Technology, Pretoria, South Africa

⁴Department of Civil and Chemical Engineering, University of South Africa, Johannesburg, South Africa

*E-mail: kkalaneme@gmail.com

Received: 29 April 2014 / Accepted: 24 June 2014 / Published: 16 July 2014

The corrosion and wear behaviours of Al matrix hybrid composites prepared using bamboo leaf ash and alumina as reinforcements were investigated in chloride medium. Alumina samples added with 2, 3, and 4 wt% bamboo leaf ash (BLA) were utilized to prepare 10 wt% of the reinforcing phase with Al-Mg-Si alloy as matrix using double stir casting process. Electrochemical studies and wear tests were performed to assess the behaviours of the composites in 3.5% NaCl. The wear and corrosion mechanisms were established with the aid of scanning electron microscopy. The analyses of the results obtained show that the corrosion resistance of the composites decreased with BLA addition in 3.5 % NaCl solution. Preferential dissolution of the more anodic Al-Mg-Si alloy matrix around the Al-Mg-Si matrix/ BLA/Al₂O₃ particle interfaces was identified as the primary corrosion mechanism. The coefficient of friction and consequently, the wear rate of the hybrid composite containing 4 wt % BLA was observed to be the highest among the composite samples produced. The single alumina reinforced and the hybrid composites containing 2 and 3 wt % BLA had comparable wear rates with the hybrids showing slightly superior wear resistance.

Keywords: Al-Mg-Si alloy, alumina, bamboo leaf ash, hybrid composites, corrosion mechanism, wear.

1. INTRODUCTION

The design of low cost aluminium matrix composites (AMCs) using cheap reinforcing materials has continued to gather interest from researchers [1-2]. Aluminium matrix composites are

well acclaimed to have found great use in the production of a wide range of products applied in automobiles, aircraft, marine, defence, sports and recreational facilities [3-5]. They are noted for their remarkable combination of a broad spectrum of properties among which are high specific strength and stiffness, good high temperature mechanical properties, excellent thermal and heat management potentials, a low coefficient of expansion, good tribological properties and satisfactory corrosion resistance [6-7]. AMCs also have the advantage of low processing cost using techniques commonly employed for the production of metals and alloys [8].

Currently, there have been efforts tailored to producing low cost AMCs, and the use of ashes produced from controlled burning of agro-wastes as reinforcement is receiving serious considerations [9-10]. Agro waste products such as baggasse, rice husk, bamboo leaves, groundnut, and coconut shell among many others after harvesting are usually discarded in the environment due to poor recycling technologies and awareness leading to diverse environmental challenges [11]. Thus research efforts targeted at converting these agro-waste products to productive uses will be of great appeal to the scientific and technological community particularly in developing countries where the effects of poor environmental waste management strategies are highly felt.

The major characteristics of AMCs developed with the use of single reinforcement derived from agro-wastes and the fact that marginal improvement in mechanical properties are achieved with their use have been reported in literatures [10-11]. In the same vein, hybrid reinforced AMCs developed utilizing agro-waste ashes and silicon carbide/alumina as complementing reinforcements have been reported to have encouraging mechanical properties depending on the weight ratio, overall weight percent, and type of the reinforcing materials used [12-13]. Rice husk ash for instance, when used as a complementing reinforcement to alumina in AMCs has been reported to have good potentials for use in stress bearing applications [12]. Other agro waste ashes such as baggasse and coconut shell have also been reported in literatures as having the potentials of serving as good reinforcements in AMCs [9]. Although a few research findings on the technological use of bamboo leaf ash have been reported in literatures [14-15]; studies devoted to the use of bamboo leaf ash as single reinforcement or complementing reinforcement to alumina/silicon for the development of low cost AMCs can hardly be found. Bamboo trees are very plentiful in the rain forest geographical region of Nigeria and are reported to be well distributed in terms of spread in most parts of the world [14]. This research work investigates the corrosion and wear behaviours of bamboo leaf ash-alumina hybrid reinforced Al-Mg-Si alloy matrix composites. This study is motivated by the prospect of developing low cost AMCs suitable for use in engineering applications where high corrosion and wear properties are desired.

2. MATERIALS AND METHOD

2.1. Materials

Al-Mg-Si alloy with chemical composition presented in Table 1 was selected as Al matrix for this study. Alumina (Al_2O_3) particles having average particle size of $28\mu\text{m}$ and bamboo leaf ash ($<50\mu\text{m}$) processed by controlled burning of dry bamboo leaves were used as reinforcement for the Al-

Mg-Si matrix. Magnesium for improving wetting between the Al-Mg-Si matrix and the reinforcements during melting was also procured.

Table 1. Elemental composition of Al-Mg-Si alloy

Element	wt%
Si	0.4002
Fe	0.2201
Cu	0.008
Mn	0.0109
Mg	0.3961
Cr	0.0302
Zn	0.0202
Ti	0.0125
Ni	0.0101
Sn	0.0021
Pb	0.0011
Ca	0.0015
Cd	0.0003
Na	0.0009
V	0.0027
Al	98.88

2.2. Preparation of bamboo leaf ash (BLA)

The bamboo leaf ash was prepared following procedures and precautions reported by Alaneme et al [12]. Dry bamboo leaves collected from farm lands having large mass of bamboo trees within the Akure metropolis (Southwest Nigeria) were used to prepare the ash. The bamboo leaves were placed in a metallic drum and fired in open air to allow for complete combustion. The ash produced from the burning process was allowed to cool for 24 hours before removal from the drum. The ash was then conditioned using a muffle furnace at a temperature of 650° C for 3 hours. A sieve shaker was used to sieve the bamboo leaf ash to obtain ashes with mesh size under 50µm. The nominal chemical composition of the bamboo leaf ash is presented in Table 2.

Table 2. Chemical composition of the bamboo leaf ash

Compound constituents	SiO ₂	Al ₂ O ₃	CaO	MgO	K ₂ O	Fe ₂ O ₃	TiO ₂
Weight percent	75.9	4.13	7.47	1.85	5.62	1.22	0.20

2.3. Production of composites

A two-step stir casting process as described by Alaneme and Aluko [16], was adopted for the production of the composites. Charge calculation was used to determine the amount of bamboo leaf ash (BLA) and alumina (Al_2O_3) required to prepare 10 wt% reinforcements (in the Al-Mg-Si alloy matrix) consisting of 0:10, 2:8, 3:7, and 4:6 bamboo leaf ash and alumina weight percentages respectively. The bamboo leaf ash and alumina particles were initially preheated separately at a temperature of 250°C to remove moisture content and to improve wettability with the molten Al-Mg-Si alloy. The Al-Mg-Si alloy billets were charged into a gas-fired crucible furnace (fitted with a temperature probe), and heated to a temperature of $750^\circ\text{C} \pm 30^\circ\text{C}$ (above the liquidus temperature of the alloy) to ensure that the alloy melts completely. The liquid alloy was then allowed to cool in the furnace to a semi solid state at a temperature of about 600°C . The preheated bamboo leaf ash and alumina particles along with 0.1 wt% magnesium were then charged into the melt at this temperature and stirring of the slurry was performed manually for 5-10 minutes. The composite slurry was superheated to $800^\circ\text{C} \pm 50^\circ\text{C}$ and a second stirring performed using a mechanical stirrer at a speed of 400rpm for 10 minutes before casting into prepared sand moulds inserted with chills. The designations used to represent each composition of the composites produced are presented in Table 3.

2.4. Corrosion test

The composite samples prepared were subjected to electrochemical method to evaluate their corrosion behaviour using potentiodynamic polarization and open circuit potential (OCP) measurements. The experiments were carried out using a Princeton applied research Potentiostat (VersaSTAT 400) with versa STUDIO electrochemical software. The experiments were performed using a three-electrode corrosion cell set-up comprising the sample as the working electrode, saturated silver/silver chloride as reference electrode, and platinum rod as counter electrode. The working electrodes were prepared by attaching an insulated copper wire to one face of the sample using an aluminum conducting tape, and cold mounting it in resin. The surfaces of the samples were wet ground with silicon carbide papers from 220 down to 600 grade (in accordance with Alaneme and Bodunrin [17] and ASTM [18] standard), washed with distilled water, degreased with acetone and dried in air. The electrolyte for the investigation was 3.5% NaCl solution and the corrosion tests were conducted at room temperature (25°C). The open-circuit corrosion potential (OCP) measurements were carried out in a separate cell for 30 hours. Potentiodynamic polarization measurements were carried out using a scan rate of 1.6 mV/s at a potential initiated at -200mV to + 1500mV with respect to OCP. After each experiment, the electrolyte was replaced, while the test samples were polished, rinsed in water and washed with acetone to remove the products that might have formed on the surface which could affect the measurement. Three repeat tests were carried out for all composition of the composites, and the reproducibility and repeatability were observed to be good as there were no significant differences between results from triplicates.

2.5. Wear Test

The wear behaviour of the single and hybrid reinforced Al-Mg-Si alloy matrix composites were tested using a CETR UMT-2 Tribometer. A load of 25N was used for 1000s, at a speed of 5Hz; and the variation of coefficient of friction with time was recorded.

2.6. Scanning electron microscopy (SEM)

In order to establish the likely corrosion mechanisms, the surface morphology of the single and hybrid reinforced Al-Mg-Si alloy matrix composite samples were characterized after immersion in 3.5% NaCl solution using a JSM 7600F Jeolultra-high resolution field emission gun scanning electron microscope (FEG-SEM).

3. RESULTS AND DISCUSSION

3.1. Electrochemical studies

The variation in the open circuit potentials as function of time for each of the composites containing varying contents of BLA exposed to 3.5% NaCl solution is presented in Figure 1. It can be observed from the plots that all the samples displayed similar OCP trends characterized by fluctuating open circuit potential profiles. This fluctuating behaviour can possibly be attributed to the simultaneous film formation and breakdown on the composites in this medium [19]. The hybrid composites B (Al-Mg-Si/ 2 wt % BLA-8 wt % Al_2O_3) and C (Al-Mg-Si/ 3 wt % BLA-7 wt % Al_2O_3) however displayed relatively stable open circuit potential patterns in comparison with the single reinforced Al-Mg-Si/ 10 wt% Al_2O_3 composite (sample A) and the hybrid composite Al-Mg-Si/ 4 wt % BLA-6 wt % Al_2O_3 (sample D). This is the case judging from the open circuit potential values of the composites sample B and C which did not show any significant increase or decrease with exposure times. The observed relatively constant potential values suggest that oxide layers of the composites sample B and C were more resistance to the attack in 3.5% NaCl solution. Also, it can be observed that the open circuit potentials of the composites were shifted to higher values with increasing BLA addition up to 3 wt% (up to sample C). This demonstrates that the addition of BLA decreased the thermodynamic tendencies of the composites to corrode. Further increase in BLA addition to 4 wt % (sample D) resulted in a drop in open circuit potential values below that of the single reinforced Al-Mg-Si/10 wt % Al_2O_3 composite. This implies a significant increase the thermodynamic susceptibility of the composite (sample D) to corrode in 3.5% NaCl solution in comparison to the other hybrid reinforced composites containing 2 and 3 wt% BLA (samples B and C).

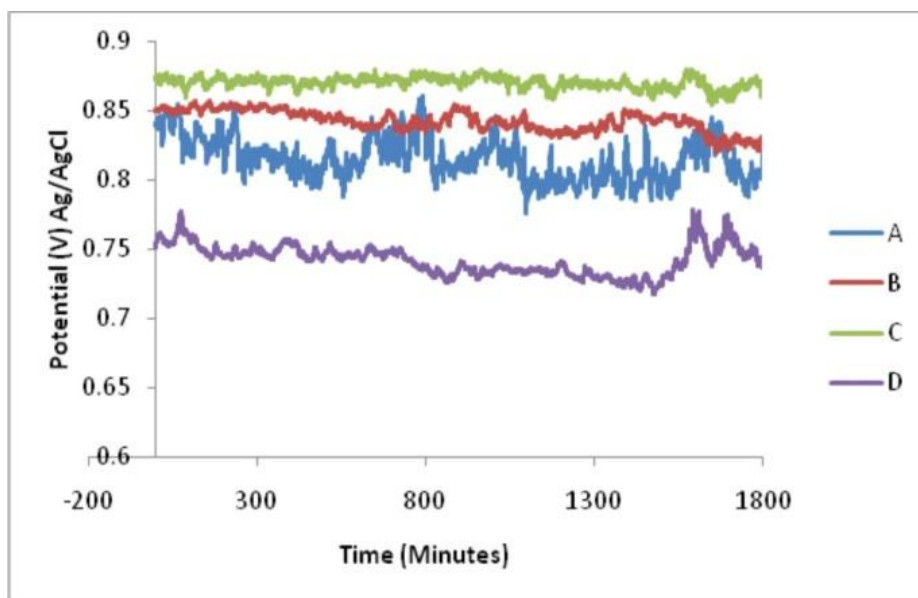
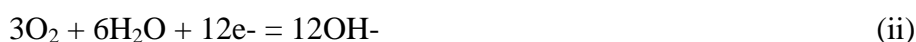


Figure 1. Variation of the open circuit potential with time for the single reinforced Al-Mg-Si/10 wt% Al₂O₃ and hybrid reinforced Al-Mg-Si/BLA-Al₂O₃ composites in 3.5% NaCl solution.

The potentiodynamic polarization curves for the composites in 3.5% NaCl solution (Figure 2) provide more information to fully comprehend the corrosion behaviour of the composites. From Figure 2, it is observed that the composites displayed similar polarization curves and passivity characteristics. The corrosion potentials (E_{corr}) of the composites are distinctly defined in the ranges of 0.7 to 0.85 mV, signifying comparatively high corrosion potentials. It can also be observed from the curves that above the Tafel region for each of the composite, a relatively constant region in the current density with increasing applied voltage was observed. This signifies the possibility of the alloys forming passive layers.

The basic anodic and cathodic reactions of aluminium in dilute HCl are dissolution of aluminium and reduction of the dissolved oxygen as shown in the equations below:



Therefore, Al³⁺ reacted with OH⁻ to form aluminium hydroxide on the surface of the aluminium as shown in equation (iii)



This hydroxide precipitated on the surface of the surface of the aluminium and gradually changed to aluminium oxide which resulted in the formation of the passive film on the surface of the aluminium as shown in equation (iv) [20].



Literature has shown that this oxide film does not offer sufficient protection against aggressive anions such as chlorides [21], hence the presence of alumina and the bamboo leaf ash provided more inhibition to suppress the dissolution of the substrate that might have initiated by the aggressive chloride ions.

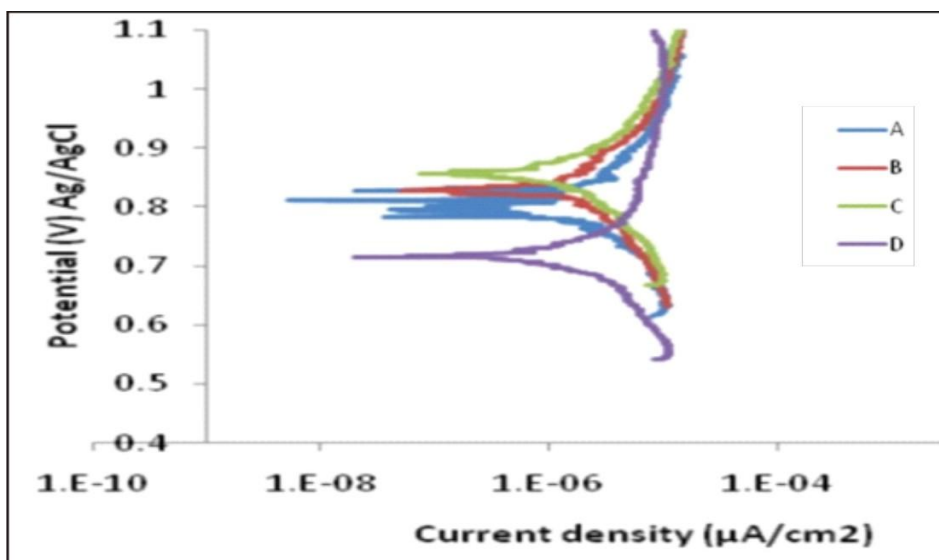


Figure 2. Potentiodynamic polarization curves for the single reinforced Al-Mg-Si/10 wt% Al₂O₃ and hybrid reinforced Al-Mg-Si/BLA-Al₂O₃ composites in 3.5% NaCl solution.

However, Table 3 which presents the corrosion potential (E_{corr}) and corrosion current density (I_{corr}) data, shows clearly that the corrosion potentials (E_{corr}) of the composites increased with increase in BLA content up to 3 wt% BLA (from sample A-C) as was the case with the OCP curves (Figure 1). But the corrosion current density (I_{corr}) also increases with increase in BLA content up to 3 wt% BLA. This signifies that, though from thermodynamics view point the stability of the composites appears to increase with BLA content up to 3 wt% (as informed by the increasing corrosion potentials to more positive values with the BLA content), the corrosion rates actually increased (from kinetics point of view and judging from the increasing corrosion current values) with the BLA addition. It should also be noted that in NaCl solution, single reinforced Al matrix - alumina composites have been reported to exhibit very good corrosion resistance in comparison to monolithic Al alloys [17]. Further addition of BLA to 4 wt% (sample D) made the composite the most susceptible to corrosion by decreasing the corrosion potential below that of the other three composites. It also increased the corrosion current. This implies that both from thermodynamics and kinetics considerations, sample D containing 4 wt % BLA is the most susceptible to corrosion of the composites produced. It should be noted that although increasing BLA content to 4 wt% (sample D) increased the susceptibility of the composite to corrosion, it is however observed that it passivated higher than the other composites with highest passivity region (Figure 2).

Table 3. Corrosion potentials and corrosion current densities of the composites

Sample Designation	Weight Ratio of BLA and Al ₂ O ₃	E_{corr} (mV)	I_{corr} (µA/cm ²)
A	0:10	799.439	1.936

B	2:8	839.256	4.13
C	3:7	853.813	4.15
D	4:6	715.318	5.583

In MMCs, localized corrosion has been identified to be the most dominant corrosion mechanism due to the presence of physical or chemical heterogeneity such as reinforcement/matrix interface, defect, intermetallic, mechanically damaged region, grain boundary, inclusion, or dislocation; where corrosion can be preferentially initiated [22-23]. This is evidenced by pits or microcrevices found in the matrix near the particle-matrix interface and from regions where there is particle dropout in alumina reinforced AMCs [19]. The SEM images (Figures 3a, b, c and d) confirm that preferential dissolution of the more anodic Al-Mg-Si alloy matrix occurs around the Al-Mg-Si matrix/ BLA/Al₂O₃ particle interfaces.

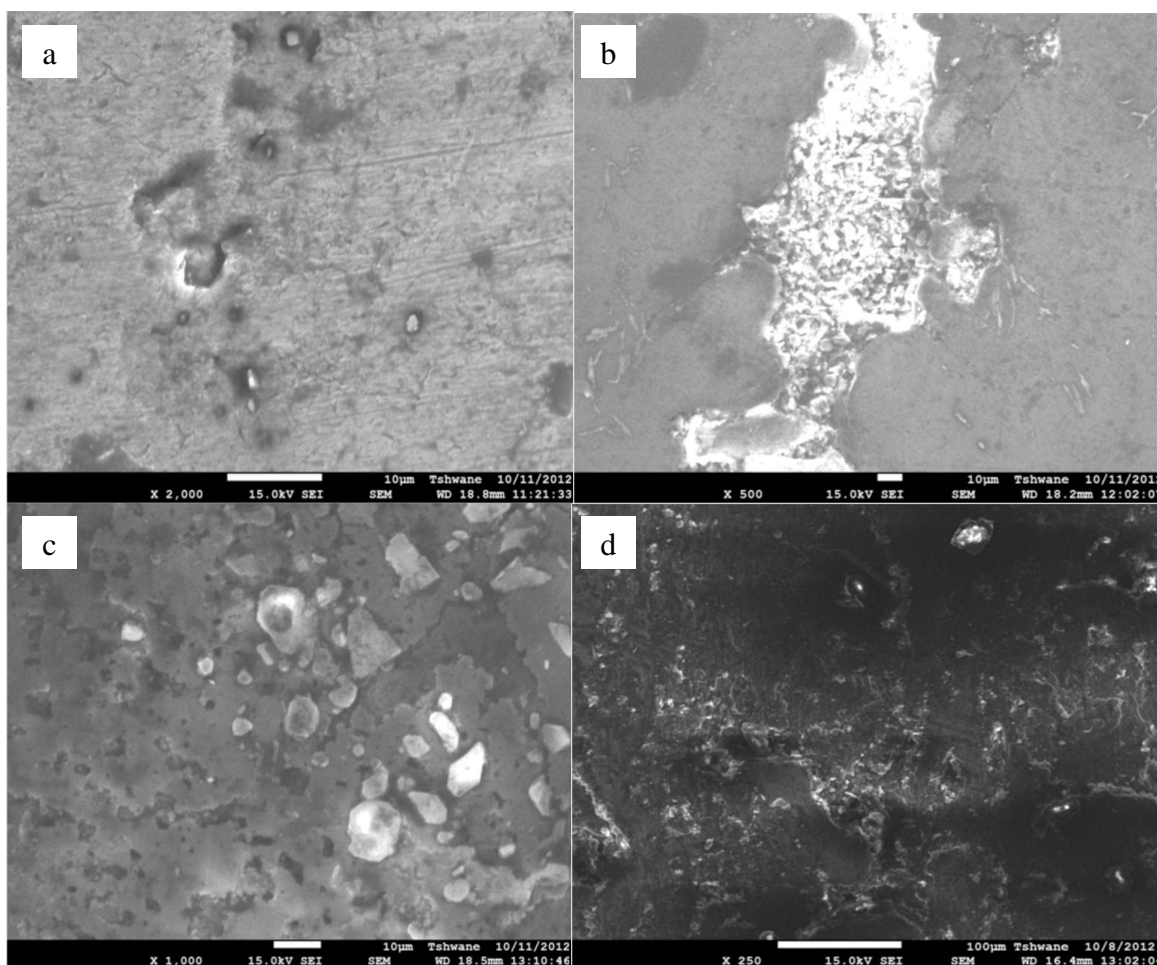


Figure 3. SEM images of the corroded surfaces of the (a) single reinforced Al-Mg-Si/10 wt% SiC composite (b) hybrid reinforced Al-Mg-Si/2 wt% BLA- 8wt% Al₂O₃ composite (c) hybrid reinforced Al-Mg-Si/3 wt% BLA- 7wt% Al₂O₃ composite, and (d) hybrid reinforced Al-Mg-Si/4 wt% BLA- 6wt% Al₂O₃ composite; after the electrochemical test in 3.5 % NaCl solution.

3.2. Wear Behaviour

The variations of coefficient of friction with time for the composites produced are presented in Figure 4. For all the composites it is observed that the friction coefficients fluctuated with time for the entire duration of the wear test. On assessment of the profiles, it is clearly seen that the Al-Mg-Si/4wt%RHA-6wt%Al₂O₃ hybrid composite (sample D) has the highest coefficient of friction in comparison to the single reinforced Al-Mg-Si matrix-10wt% Al₂O₃ composite (sample A) and the hybrid composites containing 2 and 3wt% BLA (samples B and C). This is a clear indication that the Al-Mg-Si matrix hybrid composite containing 4wt % BLA will have a higher wear rate in comparison with the other composites. Observe also that the coefficient of friction of the Al-Mg-Si/4 wt % BLA-6 wt % Al₂O₃ composite increased with time after 600 seconds of conducting the wear test. This is due to an increase in the amount of debris from the composite which adheres to the surface of the composite resulting in increase in the friction coefficient with contact time [24]. The single reinforced Al-Mg-Si matrix -10wt% Al₂O₃ composite (sample A) and the hybrid composites containing 2 and 3 wt % BLA (samples B and C) had comparable low levels of coefficient of friction. The low coefficient of friction implies that the composites (samples A, B, and C) would undergo more of abrasive wear and less plastic deformation in comparison to the hybrid composite containing 4 wt % BLA [25].

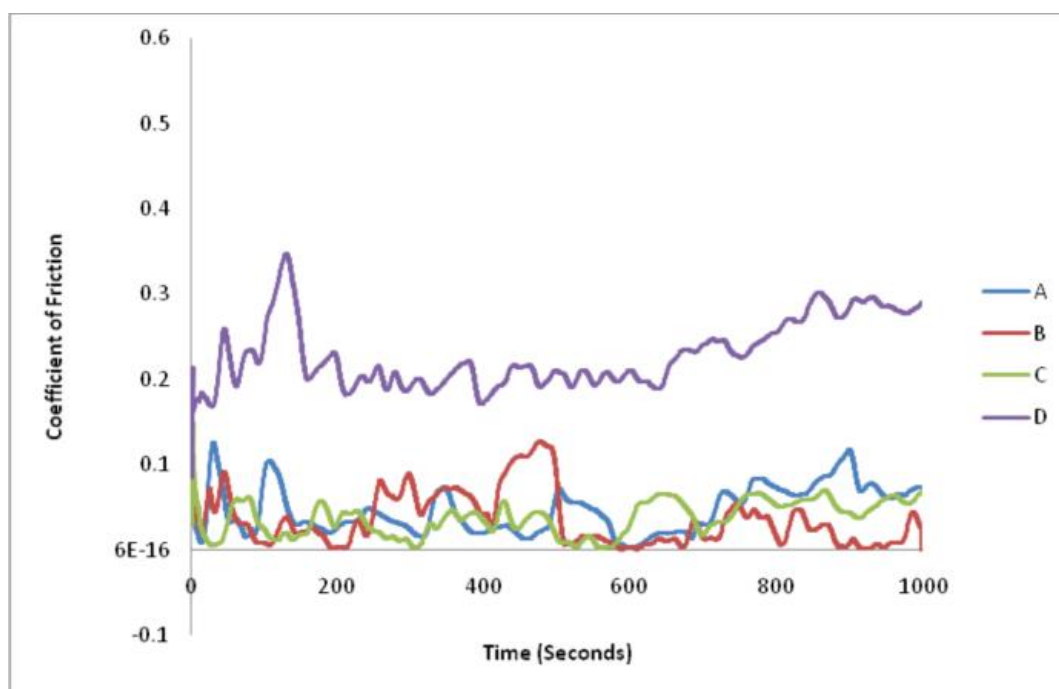


Figure 4. Variation of coefficient of friction with time for the single reinforced Al-Mg-Si/10 wt% Al₂O₃ and hybrid reinforced Al-Mg-Si/BLA- Al₂O₃ composites

The wear mechanisms proposed above are confirmed by the SEM images of the worn tracks of the composites (Figure 5). Detailed examination of the wear track of the single reinforced Al-Mg-Si matrix -10wt% Al₂O₃ composite (sample A), and the hybrid composites containing 2 and 3 wt % BLA

(samples B and C) (Figure 5a, 5b and 5C) reveal surface topographic features usually associated with a dominant abrasive mechanism. It is evident that the extent of adhesive wear is low compared to abrasive wear as there are few signs of worn debris attached to the surface of the samples. In the case of the hybrid composite containing 4 wt % BLA (Figure 5d), the surface topographic features shows large accumulation of debris on the surface of the sample arising from partial welding of the debris to the surface of the composite. The adhesion of the debris to the surface of the composite is largely responsible for the higher friction coefficients in comparison with the other composites [26-27].

It is interesting to note from Figure 4 that towards the end of the wear test (above 700 seconds), the coefficient of friction of the single reinforced composite (sample A) was slightly higher than that of the hybrid composites samples B and C (Figure 4). This suggests that overall the hybrid composites samples B and C may be slightly more wear resistant than the single reinforced composite (sample A).

The results from the test are quite revealing as it shows the promise of the cheaply produced BLA-alumina hybrid reinforced Al-Mg-Si alloy matrix composites for wear applications.

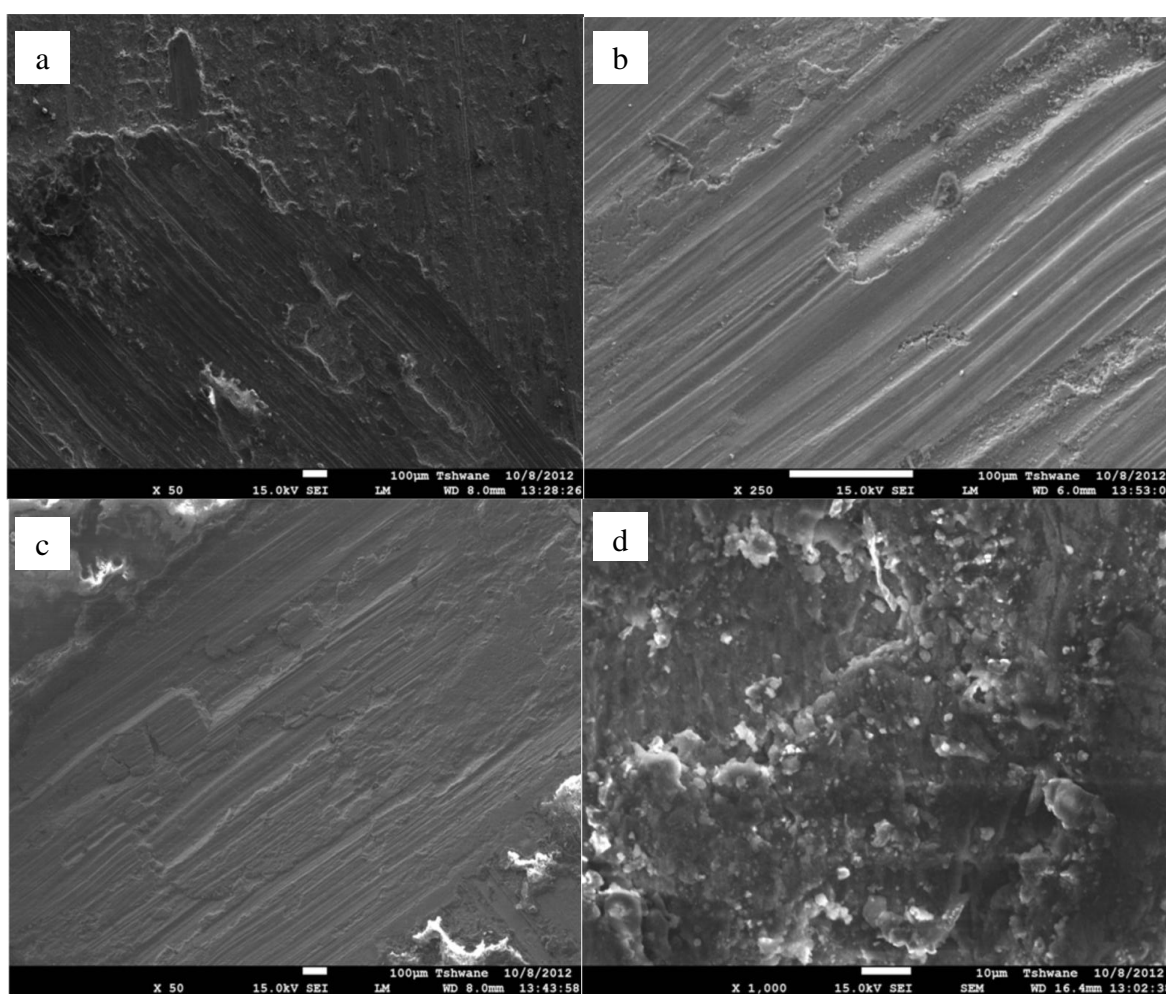


Figure 5. SEM images of the worn surfaces of the (a) single reinforced Al-Mg-Si/10wt% Al_2O_3 composite (b) hybrid reinforced Al-Mg-Si/2wt%BLA-8wt% Al_2O_3 composite (c) hybrid reinforced Al-Mg-Si/3wt%BLA-7wt% Al_2O_3 composite, and (d) hybrid reinforced Al-Mg-Si/4wt% BLA-6wt% Al_2O_3 composite.

4. CONCLUSIONS

The corrosion and wear behaviour of Al-Mg-Si matrix composites containing 0:10, 2:8, 3:7, and 4:6 wt% of bamboo leaf ash and alumina as reinforcement was investigated. The analyses of the obtained results showed that:

1. The corrosion resistance of the composites decreased with BLA addition in 3.5% NaCl solution.
2. Preferential dissolution of the more anodic Al-Mg-Si alloy matrix around the Al-Mg-Si matrix/ BLA/Al₂O₃ particle interfaces was identified as the primary corrosion mechanism.
3. The coefficient of friction and consequently, the wear rate of the hybrid composite containing 4 wt% BLA was observed to be higher than that of the composites produced. The single reinforced and hybrid composites containing 2 and 3 wt% BLA had comparable wear rates with the hybrids showing slightly superior wear resistance.
4. The production of low cost Al-Mg-Si alloy matrix hybrid composites using bamboo leaf ash as a complementing reinforcement to alumina shows great promise for wear resistance applications judging from the good wear properties exhibited by the hybrid composites containing 2 and 3 wt % BLA.

References

1. H. Zuhailawati, P. Samayamutthirian, C.H. MohdHaizu, *Journal of Physical Science*, 18(1) (2007) 47.
2. K.V. Mahendra, A. Radhakrisna, *Journal of Composite Materials*, 44(8) (2010) 989.
3. K.K. Alaneme, *International Journal of Mechanical and Materials Engineering*, 7(1) (2012) 96.
4. P. Rohatgi, B. Schultz, *Materials Matters*, 2 (2007)16.
5. A. Macke, B.F. Schultz, P. Rohatgi, *Advanced Materials and Processes*, 170(30) (2012)19.
6. K.K. Alaneme, A.O. Aluko, *Scientia Iranica, Transactions A: Civil Engineering (Elsevier)*, 19(4) (2012) 992.
7. T.V. Christy, N. Murugan, S. Kumar, *Journal of Minerals and Materials Characterization and Engineering*, 9(1) (2010) 57.
8. D.B. Miracle, *Composites Science and Technology*, 65(15/16) (2005) 2526.
9. P.B. Madakson, D.S. Yawas, A. Apasi, *International Journal of Engineering Science and Technology (IJEST)*, 4(3) (2012)1190.
10. S.D. Prasad, R.A. Krishna, *International Journal of Advanced Science and Technology*, 33 (2011)51.
11. M.A. Maleque, A. Atiqah, R.J. Talib, H. Zahurin, *International Journal of Mechanical and Materials Engineering*, 7(2) (2012)166.
12. K.K. Alaneme, I.B. Akintunde, P.A. Olubambi, T. M. Adewale, *Journal of Materials Research and Technology*, 2(1) (2013)60-67.
13. R. Escalera-Lozano, C. Gutierrez, M.A. Pech-Canul, M.I. Pech-Canul, *Waste Management*, 28 (2008)389.
14. O.A. Nwoke, B.O. Ugwuishiwu, *International Journal of Sustainable Construction Engineering and Technology*, 2(2) (2011) 2180.
15. O.O. Amu and A.A. Adetuberu, *International Journal of Engineering and Technology*, 2(4) (2010)212.
16. K.K. Alaneme, A.O. Aluko, *West Indian Journal of Engineering*, 34(1/2) (2012) 80.

17. K.K. Alaneme, M.O. Bodunrin, *Journal of Minerals and Materials Characterisation and Engineering*, 10(2) (2011)1153.
18. ASTM, G5-94(2004): Annual book of ASTM standards, Standard reference test method for making potentiostatic and potentiodynamic anodic polarization measurements, 2004.
19. B. Bobic, S. Mitrovic, M. Bobic, I. Bobic, *Tribology in Industry*, 32(1) (2010) 3.
20. B. Gao, X. Zhang, Y. Sheng, *Materials Chemical Physics*, 108 (2008) 375.
21. R. Rosliza, W.B. Wan Nik, *Current Applied Physics*, 10 (2010) 221.
22. K.K. Alaneme, *Leonardo Journal of Science*, 18 (2011)55.
23. A.J. Dolata, M. Dyzia, W. Walke, *Solid State Phenomena*, 191(2012) 81.
24. K. Ravi Kumar, K.M. Mohanasundaram, G. Arumaikkannu, R. Subramanian, *Tribology Transactions*, 55(6) (2012)723.
25. S. Suresha, B.K. Sridhara, *Materials and Design*, 34(2012) 576.
26. V. Gaitonde, S. Karnik, M. Jayaprakash, *Journal of Minerals and Materials Characterization and Engineering*, 11(7) (2012)695.
27. A. Onat, *Journal of Alloys and Compounds*, 489(2010)119.

© 2014 The Authors. Published by ESG (www.electrochemsci.org). This article is an open access article distributed under the terms and conditions of the Creative Commons Attribution license (<http://creativecommons.org/licenses/by/4.0/>).